Water Resources Research

REVIEW ARTICLE
10.1029/2023WR035053

Formulations and Diffusivity Coefficients of the 2D Depth-Averaged Advection-Diffusion Models: A Literature Review

Emmanuel Mignot[1], Nicolas Riviere[1], and Benjamin Dewals[2]

[1]LMFA, University of Lyon, INSA Lyon, CNRS, Ecole Centrale Lyon, Université Claude Bernard Lyon and UMR5509, Villeurbanne, France, [2]Hydraulics in Environmental and Civil Engineering (HECE), University of Liège (Uliège), Liège, Belgium

Key Points:

- Several formulations of the 2D advection-diffusion equations are being used by different authors in the literature
- Several formulations and coefficient values of the diffusivity tensor are employed
- The number and quality of the available validation data sets are too weak, which limits the validation processes performed by the authors

Supporting Information:

Supporting Information may be found in the online version of this article.

Correspondence to:

E. Mignot,
Emmanuel.mignot@insa-lyon.fr

Citation:

Mignot, E., Riviere, N., & Dewals, B. (2023). Formulations and diffusivity coefficients of the 2D depth-averaged advection-diffusion models: A literature review. *Water Resources Research*, *59*, e2023WR035053. https://doi.org/10.1029/2023WR035053

Received 4 MAY 2023
Accepted 17 NOV 2023

Author Contributions:

Conceptualization: Emmanuel Mignot
Formal analysis: Nicolas Riviere
Investigation: Emmanuel Mignot, Benjamin Dewals
Methodology: Emmanuel Mignot
Resources: Benjamin Dewals
Supervision: Emmanuel Mignot
Validation: Nicolas Riviere
Writing – original draft: Emmanuel Mignot
Writing – review & editing: Benjamin Dewals

Abstract This article reviews the mathematical formulations of the depth-integrated advection-diffusion equation used so far for modeling scalar transport and mixing in shallow environmental flows. It also summarizes the main approaches developed to evaluate the diffusivity tensor in such models. Remarkably, seven different formulations were found for the depth-averaged advection-diffusion equation, and eight distinct approaches have been used for determining the coefficients of the diffusivity tensor. Besides, only a minority of the reviewed studies report calibration of the diffusivity tensor against experimental or field observations. The fragmentation of existing methodologies exhibits a lack of scientific consensus. Promising approaches are highlighted and possible paths for improving the calibration, validation and transferability of the diffusivity coefficients are outlined.

1. Introduction

Applications of the simulation of particulate or dissolved matter mixing in shallow watercourses, sewers, or flooded streets are multiple and of high relevance for addressing timely environmental and societal challenges. Worldwide, point source releases of pollutants from industries, from water-based cooling systems, or from wastewater treatment plants (e.g., Morales-Hernandez et al., 2019) heavily impact rivers and estuaries. Simulating the fate of these contaminants is of critical importance to support their monitoring and for environmental management. Similarly, accurately predicting the mixing of accidently released pollutants in rivers and coastal areas is instrumental to inform pollution control strategies and environmental protection (Li & Duffy, 2012; Park et al., 2020). Flood events affecting urbanized floodplains may damage wastewater treatment plants or other facilities that have the potential to release pollutants in the environment (Fang et al., 2022; Murillo et al., 2006). Release of pollutant during urban floods may also result from surcharging sewer systems (Sämann et al., 2019). This adversely affects public health and may worsen the impacts in already devastated areas (Addison-Atkinson et al., 2022; Mark et al., 2018; Zhang et al., 2015). Accurate modeling of mixing effects is also important for setting up more advanced diagnostic tools such as based on characteristic time scales (e.g., pollutant age, retention time or transit time), which are decisive for evaluating the ecological impacts of pollutants in streams and coastal areas.

Computing scalar transport and mixing in open-channel flows is usually performed in two steps. First, a hydrodynamic model is used to predict the velocity and water depth fields. Second, an advection-diffusion model is solved to compute the spatial distribution of scalar concentration. It is standard, indeed, to consider this one-way coupling between the two models. In general, resolving the flow field requires 3D models but when the flow is shallow enough, a common simpler approach consists in solving the 2D shallow-water equations for the flow and a 2D-horizontal advection-diffusion equation for the transport and mixing of the scalar. In a typical laterally bounded shallow flow configuration, such as in a river, the relative importance of vertical, streamwise and cross-wise mixing varies according to the distance to the location of scalar injection (Baek & Seo, 2010; Gualtieri, 2010). In the near-field of the scalar injection location, vertical mixing is important and predicting the scalar transport and mixing requires 3D calculations. Conversely, in the mid-field, the vertical gradients of scalar concentration vanish so that the 2D-horizontal assumption applies and solving the 2D-horizontal advection-diffusion equation is sufficient. Finally, in the far-field, lateral mixing is fully achieved (the concentration becomes homogeneous throughout the flow cross-section), and only longitudinal mixing still influences the concentration distribution. This situation can be simplified to as a 1D streamwise problem. The present work focusses on the "mid-field" configuration, far enough from the source but still in a region where transverse mixing has an influence.

Transport and mixing in many environmental flows may be described based on a 2D-horizontal depth-averaged advection-diffusion model. This is notably the case for contaminant, nutriment, or fine sediment mixing in rivers or canals including the corresponding singularities (Jakson et al., 2013) such as confluences, bifurcations, cavities, the overflows in floodplains, flooded urban areas, pressurized sewers, shallow ponds as well as deltas and coastal areas.

Predicting flow depths and velocity fields in shallow flows using the 2D shallow-water equations has become of common practice and the model outcomes are trusted with a high level of confidence for a broad range of configurations. In contrast, no consensus exists on the most suitable method to parametrize the effects of turbulent diffusion and dispersion (induced by velocity shear and secondary currents) in the 2D depth-averaged advection-diffusion equation. The approaches used so far for selecting the value of coefficients in the corresponding 2D diffusivity tensor are multiple and fragmented. This article reviews the variety of formulations of the 2D depth-averaged advection-diffusion equation used by the previous works in the literature and of formulations of the corresponding diffusivity tensor, leaving apart a review of the available analytical solutions. Indeed, these solutions are often based on simplifying assumptions—such as constant-depth and one-dimensional flows. In Section 2, the mathematical formulations of the depth-averaged advection-diffusion equations used in the 28 reviewed studies are introduced, and the implications of variations in the model formulation are discussed. Section 3 summarizes the various considered approaches for estimating the form of the diffusivity tensor and the values of the constitutive diffusivity coefficients. The differences between the reviewed studies are discussed in Section 4, and conclusions are drawn in Section 5.

2. Depth-Integrated Mathematical Model

2.1. Governing Equation

The 2D depth-averaged advection-diffusion equation is obtained by integrating over the flow depth (vertical axis) the 3D advection-diffusion equation (Equation A3 in Supporting Information S1). This equation (equivalent to Equation A12 in Supporting Information S1) reads:

$$\frac{\partial}{\partial t}(hC) + \mathrm{div}(h\,\mathbf{U}C) + \underbrace{\mathrm{div}\left[h\left\langle\left(\overline{\mathbf{u}}-\mathbf{U}\right)\left(\overline{c}-C\right)\right\rangle\right]}_{\mathrm{T3}} + \underbrace{\mathrm{div}\left(-h\,\varepsilon_m\left\langle\mathrm{grad}\,\overline{c}\right\rangle\right)}_{\mathrm{T1}} + \underbrace{\mathrm{div}\left(h\left\langle-\varepsilon_t\,\mathrm{grad}\,\overline{c}\right\rangle\right)}_{\mathrm{T2}} = S \quad (1)$$

with h is the water depth; $\overline{\mathbf{u}} = [\overline{u}\ \overline{v}]^{\mathrm{T}}$, and $\mathbf{U} = [U\ V]^{\mathrm{T}}$, respectively the local and depth-averaged flow velocity vectors in the horizontal x-y plane; $\overline{c}$ and C, respectively the local and depth-averaged concentration; ε_m is the molecular diffusivity coefficient (m^2/s), ε_t is the turbulent diffusivity tensor (m^2/s), S is the depth-integral of the source (or sink) term, and div the divergence in 2D (x, y). The angle brackets denote a depth-averaged quantity, whereas an overbar refers to a Reynolds-average of a local variable (i.e., not depth-averaged). A detailed derivation of Equation 1 is given in Texts S1 and S2 in Supporting Information S1.

The last three terms in Equation 1 represent three distinct processes responsible for the scalar mixing: (a) the molecular diffusion (term labeled T1), (b) the turbulent diffusion (term labeled T2) and (c) the dispersion induced by the non-uniform distribution over the depth of both the flow velocity (velocity shear, including the effect of the coherent secondary currents) and the concentration (included in term labeled T3).

Resorting to an assumption similar to that of Boussinesq in Reynolds-averaged models, the last three terms in the left-hand side (LHS) of Equation 1 are generally parametrized as a single term so that this equation reads:

$$\frac{\partial}{\partial t}(hC) + \mathrm{div}(h\,\mathbf{U}C - h\,\mathbf{D}\,\mathrm{grad}\,C) = S \quad (2)$$

with $\mathbf{D}$ is the diffusivity tensor. A 2×2 tensor is used here because some of the processes expressed by term T2 and, to a greater extent, by term T3 are strongly direction-dependent, (e.g., in presence of secondary currents). Equation 2 can be written out in full as follows:

$$\frac{\partial}{\partial t}(hC) + \frac{\partial}{\partial x}(hUC) + \frac{\partial}{\partial y}(hVC) = \frac{\partial}{\partial x}\left[h\left(D_x\frac{\partial C}{\partial x} + D_{xy}\frac{\partial C}{\partial y}\right)\right] + \frac{\partial}{\partial y}\left[h\left(D_{yx}\frac{\partial C}{\partial x} + D_y\frac{\partial C}{\partial y}\right)\right] + S \quad (3)$$

Formally, Equations 2 and 3 look relatively simple, but comparing them with Equation 1 highlights to which extent the tensor **D** lumps processes of various natures. As such, the determination of tensor **D** for real-world applications remains particularly challenging. The coefficients D_x and D_y correspond to gradient-diffusion, also referred to as "Fickian dispersion terms" or "Fickian turbulent diffusion" (Fischer et al., 1979), while the terms involving D_{xy} and D_{yx} are referred to as "cross-dispersion terms" (Fischer, 1978; Lee & Kim, 2012).

Equations 2 and 3 are conservative since they were directly derived from the application of mass conservation. As such, they are suitable for a computational resolution with shock-capturing schemes.

2.2. Alternate Formulations

According to the review performed herein (Table 2), Equation 3 was used in most studies dedicated to 2D simulation of scalar dispersion in shallow flows. However, some variations in the model formulation were also found in our literature review. In the following paragraphs, we introduce alternate formulations used first for the LHS of Equation 3, second for the right-hand side (RHS), and third in modeling approaches assuming a constant and uniform flow depth.

2.2.1. Left-Hand Side

By combining Equation 3 with the depth-integrated continuity equation of the flow, the LHS of Equation 3 may be reformulated in a nonconservative form:

$$\text{LHS} = h\frac{\partial C}{\partial t} + hU\frac{\partial C}{\partial x} + hV\frac{\partial C}{\partial y} \tag{4}$$

Note that Formulation 4 does not imply that the flow depth should be constant nor uniform in space. However, this formulation may lead to issues with the computational resolution. The nonconservative formulation is less suitable for the application of certain families of numerical schemes such as finite volume techniques, and it makes the model ill-suited for representing the propagation of steep fronts (Ferziger & PeriC, 2002).

2.2.2. Right-Hand Side

In a limited number of studies (Duan, 2004; Fang et al., 2022; Wan et al., 2020), the dispersive fluxes are expressed as a function of the gradient of the product of the water depth and scalar concentration hC instead of the gradient of concentration C alone. Accordingly, the RHS of Equation 3 is formulated as follows:

$$\text{RHS} = \frac{\partial}{\partial x}\left[D_x\frac{\partial}{\partial x}(hC) + D_{xy}\frac{\partial}{\partial y}(hC)\right] + \frac{\partial}{\partial y}\left[D_{yx}\frac{\partial}{\partial x}(hC) + D_y\frac{\partial}{\partial y}(hC)\right] + S \tag{5}$$

In addition to the simplifications made to the RHS already discussed in Equation 5, Hu et al. (2017) consider that the diffusivity tensor is isotropic and spatially homogeneous so that the single diffusion coefficient gets out from the derivatives as:

$$\text{RHS} = D\left[\frac{\partial^2}{\partial x^2}(hC) + \frac{\partial^2}{\partial y^2}(hC)\right] + S \tag{6}$$

Formulations 5 and 6 seem questionable in terms of physical representation. Indeed, in the particular case of a uniform flow (say along direction x) in a channel with a natural transverse bathymetric profile (e.g., deeper in the center compared to near the banks) and far enough downstream from the scalar release source so that the LHS becomes nil, these formulations predict that the transverse distribution of concentration ensures that the product hC remains constant in the crosswise direction (y), that is, that the concentration would be way smaller in regions of larger flow depth near the center of the cross-section compared to (near-bank) shallower regions. This is not supported by empirical knowledge (e.g., Gond et al., 2021).

2.2.3. Constant and Uniform Flow Depth

In the case where the flow depth is assumed constant and uniform, the variable h may be moved under or out of time and space derivatives, and thus be canceled. Several authors use equations that do not involve variable h

(Alavian, 1986; Cheng et al., 1984; De Barros et al., 2006; Gualtieri, 2010; Lee & Kim, 2012). The formulation of Lee and Kim (2012) is identical to Equation 3 except for the missing variable h:

$$\frac{\partial C}{\partial t} + \frac{\partial}{\partial x}(UC) + \frac{\partial}{\partial y}(VC) = \frac{\partial}{\partial x}\left(D_x \frac{\partial C}{\partial x} + D_{xy}\frac{\partial C}{\partial y}\right) + \frac{\partial}{\partial y}\left(D_{yx}\frac{\partial C}{\partial x} + D_y \frac{\partial C}{\partial y}\right) + S \tag{7}$$

while Alavian (1986) uses a nonconservative formulation similar to Equation 4:

$$\frac{\partial C}{\partial t} + U\frac{\partial C}{\partial x} + V\frac{\partial C}{\partial y} = \frac{\partial}{\partial x}\left(D_x \frac{\partial C}{\partial x} + D_{xy}\frac{\partial C}{\partial y}\right) + \frac{\partial}{\partial y}\left(D_{yx}\frac{\partial C}{\partial x} + D_y \frac{\partial C}{\partial y}\right) + S \tag{8}$$

Despite slight variations in the expression of the RHS of the equation, the formulation used by Cheng et al. (1984) and Gualtieri (2010) is equivalent to Equation 8. De Barros et al. (2006) use a steady form of Equation 8 by canceling the time derivative in the LHS.

Finally, Wan et al. (2020) use a hybrid formulation of the advective terms, in which h is kept within the derivatives of the LHS like in Equation 3 while the depth-averaged velocity components appear out of the derivatives like in Equations 4 and 8. This leads to the following reformulation of the LHS of Equation 3:

$$\text{LHS} = \frac{\partial}{\partial t}(hC) + U\frac{\partial}{\partial x}(hC) + V\frac{\partial}{\partial y}(hC) \tag{9}$$

2.2.4. Change of Reference Frame

Cheng et al. (1984) use the following alternative formulation:

$$\frac{\partial C}{\partial t} + U\frac{\partial C}{\partial x} + V\frac{\partial C}{\partial y} = \frac{1}{h}\left[\frac{\partial}{\partial s}\left(D_L h \frac{\partial C}{\partial s}\right) + \frac{\partial}{\partial n}\left(D_T h \frac{\partial C}{\partial n}\right)\right] + S \tag{10}$$

where s and n refer to coordinates aligned with directions parallel and normal to the local flow velocity and L and T indices refer, respectively, to the longitudinal and transverse directions. Still, the RHS of Equation 10 can be rewritten as a function of x and y coordinates (see next section), leading to a formulation equivalent to the RHS of Equation 3.

3. Diffusivity Tensor

Besides variations in the formulation of the governing equations, past studies used various parameterizations for the diffusivity tensor $\mathbf{D}$. Besides simply neglecting $\mathbf{D}$ (i.e., assuming $\mathbf{D} = \mathbf{0}$), eight approaches could be identified for estimating the diffusivity tensor $\mathbf{D}$ in Equations 2, 3, 5–8 [5–8], and 10. As detailed in Table 1, the differences between these approaches are threefold.

- First, the value of either one, two, three, or four coefficients needs to be assessed for evaluating $\mathbf{D}$. These constitute the rows of Table 1.
- Second, the considered coefficients represent either (a) constant diffusivity coefficients (noted D and expressed in m^2/s, in the second column of Table 1), or diffusivity coefficients that depend on the flow characteristics. This dependency can be (b) based on Elder approach, relating the diffusivity coefficient to the product hu_* with u_* the local friction velocity (in the third column of Table 1), or (c) or based on dispersion-diffusion Schmidt numbers (noted σ_c, nondimensional and simply referred to as "Schmidt number" in the sequel) that are the ratios between the turbulent viscosity and the diffusivity coefficient (in the fourth column).
- Third, the coefficients may relate either to the directions of the Cartesian reference axes (x, y) or be linked to local and instantaneous streamwise and transverse (s, n) directions. In this case, coefficients are, usually and hereafter, marked with L and T indices.

This results in eight different approaches, which are summarized in Table 1 and labeled from ① to ⑧. Approaches ①, ②, and ③ involve just a single, isotropic coefficient, even though its physical meaning and values are different in each approach. In approach ④, two distinct coefficients are introduced along directions x and y of the frame of reference. With no off-diagonal terms, such a formulation considers only gradient-diffusion processes and thus seems sensible when the principal axis of the flow is mostly aligned with the frame axes. In contrast, the formulations adopted in approaches ⑤, ⑥, and ⑦, based on the streamwise and normal directions (s, n), enable a better

Table 1
Existing Approaches for Estimating the Diffusivity Tensor $\mathbf{D}$ *in Depth-Averaged Transport and Dispersion Models*

Number of coefficients		Dimensional diffusivity coefficient(s) (m^2/s)		Nondimensional coefficient(s) (–) describing the ratio of diffusivity to hu_* (Elder approach)		Schmidt number (–)
1	①	$\mathbf{D} = D\,\mathbf{I}$	②[a,b]	$\mathbf{D} = k\,\mathbf{R}^T\begin{pmatrix} hu_{*L} & 0 \\ 0 & hu_{*T} \end{pmatrix}\mathbf{R}$	③	$\mathbf{D} = \nu_T/\sigma_c\,\mathbf{I}$
2	④	$\mathbf{D} = \begin{pmatrix} D_x & 0 \\ 0 & D_y \end{pmatrix}$				
2	⑤[a]	$\mathbf{D} = \mathbf{R}^T\begin{pmatrix} D_L & 0 \\ 0 & D_T \end{pmatrix}\mathbf{R}$	⑥[a]	$\mathbf{D} = \mathbf{R}^T\begin{pmatrix} k_L hu_* & 0 \\ 0 & k_T hu_* \end{pmatrix}\mathbf{R}$		
3–4[c]	⑦[a]	$\mathbf{D} = \mathbf{R}^T\begin{pmatrix} D_L & D_{LT} \\ D_{TL} & D_T \end{pmatrix}\mathbf{R}$				
3–4[d]	⑧	$\mathbf{D} = \begin{pmatrix} D_x & D_{xy} \\ D_{yx} & D_y \end{pmatrix}$				

[a]Notation $\mathbf{R}$ represents a rotation matrix of an angle corresponding to the angle between the local and instantaneous streamwise direction and the x-axis, this angle being computed from the outcome of the hydrodynamic model. [b]Morales-Hernandez et al. (2019) used direction-dependent values of the friction velocity, noted here u_{*_L} and u_{*_T}. In contrast, Fang et al. (2022) used a conventional evaluation of the friction velocity u_*, so in this case $u_{*_L} = u_{*_T} = u_*$. [c]Lee and Kim (2012) considered $D_{LT} = D_{TL}$ so that only three coefficients were required. [d]Park et al. (2020) and Seo et al. (2008) used Equation 11 combined with information on the vertical profiles of velocity and a parametrization of ε_{zl} to derive space-dependent values of D_x, D_y, D_{xy}, and D_{yx}. However, Seo et al. (2008) reported that D_{xy} and D_{yx} "have almost the same values" and Park et al. (2020) considered $D_{xy} = D_{yx}$.

consideration of cases involving varying flow directions within the flow domain. With no off-diagonal terms, approaches ⑤ and ⑥ consider only gradient-diffusion processes along the main flow axes. These approaches often capitalize on existing coefficients. Note that when passing from the (s, n) to the (x, y) frame using the rotation matrix $\mathbf{R}$, off-diagonal terms appear in the diffusivity tensor (e.g., Alavian, 1986). Approach ⑦ adds a third coefficient, considering two identical off-diagonal cross-dispersion terms. Approach ⑧ involves four coefficients in the (x, y) Cartesian frame axis. The transformation of the diffusivity tensor from the local to the Cartesian frame, detailed by Lee and Kim (2012) is reproduced in Text S3 in Supporting Information S1.

Approach ① was used solely in studies which either (a) neglect the dispersion-diffusion effects (i.e., coefficient D set to zero for model application, such as Murillo et al., 2006 or Behzadi et al., 2018), (b) do not report which value is assigned to the coefficient (Gualtieri, 2010; Li & Duffy, 2012), or (c) use arbitrarily set values for the diffusivity (Pathirana et al., 2011). Approach ② was used by Fang et al. (2022) in combination with a conventional (direction-independent) evaluation of the shear velocity, resulting in an isotropic diffusivity tensor. In contrast, Morales-Hernandez et al. (2019) also considered a single coefficient, in line with approach ②, but they used direction-dependent values for the shear velocity so that the resulting diffusivity tensor was nonisotropic. In approach ③, which involves a coefficient similar to a Schmidt number, the required turbulent viscosity ν_t may be estimated from various turbulence closures used in the 2D shallow-water equations for flow computation: for example, constant turbulent viscosity, Elder formula (Duan, 2004; Hu et al., 2017), Smagorinsky formulation (Hu et al., 2017; Wan et al., 2020), or depth-averaged k-ε model (Ye & McCorquodale, 1997). For Approach ④, only De Barros et al. (2006) justified the coefficient values used in the diffusivity tensor in a straight channel so that directions $x = s$ and $y = n$. The authors neglected the longitudinal mixing ($D_x = 0$) and used a transverse D_y diffusivity coefficient value equal to D_T based on literature data. For approach ⑤, the authors best-fit their diffusivity coefficients based on laboratory data (Lee & Seo, 2007) or river data (Lee & Seo, 2007, 2010; Piasecki & Katopodes, 1999). For approach ⑥, the authors either (a) use standard values from the literature as

Water Resources Research

10.1029/2023WR035053

Table 2
Synthesis of the Equations, Diffusion Tensors, the Origin of Their Coefficients and Description of the Calibrated and Validation Experimental Data Used by the Authors

Reference	Equation	Scheme and order[a]	Diffusivity approach (Table 1)	Model verification against analytical solution	Source of diffusivity values			Independent validation by
					Values	Literature data[b]	Calibrated values	Comparison with independent measurements
a. Null diffusivity coefficient								
Murillo et al. (2006)	(3)	Fv, 1st			D set to 0			No
Behzadi et al. (2018)	(3)	Fv, 2nd	①	Yes	$D = 0.01$ for the analytical case $D = 0$ for the application case			No
b. Not reported diffusivity coefficient values								
Gualtieri (2010)	(8)		①	No	Not reported			13 mean transverse mixing coefficients from laboratory straight open-channel measurements (Lau & Krishnappan, 1977)
Li and Duffy (2012)	(3)	Fv, 2nd	①	No	D =0, 0.01, and 1 m^2/s for test cases but not reported for application case			No
Zhang et al. (2015)	(3)	Fv, 2nd	④	Yes	$D_x = 1.02$ m^2/s, $D_y = 0.094$ m^2/s for test cases but not reported for application case			No
Mark et al. (2018)	(3)		④	No	Not reported			No
Fernández-Pato and García-Navarro (2021)	(3)	Fv, 1st	④	No	Not reported			No
c. Not justified (arbitrary) diffusivity coefficient values								
Cheng et al. (1984)	(8)	Fd, 2nd	④	Yes	Idealized cases: $D_x = D_y = 0$ $D_x = 3$ m^2/s, $D_y = 0.12$ m^2/s $D_x = 10$ m^2/s, $D_y = 1$ m^2/s $D_x = D_y = 3.16$ m^2/s			No
	(10)		⑤		Field case: D_L=30 m^2/s, D_T=3 m^2/s			

Water Resources Research

10.1029/2023WR035053

Table 2
Continued

Reference	Equation	Scheme and order[a]	Diffusivity approach (Table 1)	Model verification against analytical solution	Source of diffusivity values: Values	Source of diffusivity values: Literature data[b]	Source of diffusivity values: Calibrated values	Independent validation by: Comparison with independent measurements
Alavian (1986)	(8)	Fe, 2nd	⑤	No	$D_L = 0.05$ m^2/s, $D_T = 0.1$–$1\ D_L$			No
Lin and Falconer (1997)	(3)	Fd, 3rd	⑥	Yes	$D_L = 13hu_*D_T = 1.2hu_*$			2 time-evolution signals of sediment flux measured in the Humber (UK) estuary by British Transport Docks Board (1980)
Pathirana et al. (2011)	(3)	Fv, 1st	①	Yes	$D \sim 0.06$ m^2/s or 0.05 m^2/s (adjusted with the cell size)			No
Lee and Kim (2012)	(7)	Fe	⑤	No	D_L=0.005 m^2/s, D_T=0.001 m^2/s, D_{LT}= D_{TL}= –0.002 m^2/s or D_{LT}= D_{TL}= 0 m^2/s			No
			⑦		D_L=0.01 m^2/s, D_T = 0.001 m^2/s, D_{LT}= D_{TL}=–0.002 m^2/s or D_{LT}= D_{TL}=0 m^2/s			
Wan et al. (2020)	LHS: (9) RHS: (5)		③[c]	No	$\sigma_c = 1$			4 locations of total dissolved gas saturation measured in the Jinsha river (China)
d. Coefficients taken from the literature								
Falconer (1986)	(3)	Fd, 2nd	⑥	No	$D_L = 5.93hu_*$ $D_T = 0.15hu_*$	Elder (1959), Fischer (1973)		24 measured location of nitrogen concentration in the inland basin of Poole (UK)
De Barros et al. (2006)	(8) *steady*	2nd	④	No	$D_x = 0$ m^2/s $D_y = 0.05$ m^2/s	Fischer et al. (1979) and user's Guide for RIVRISK (2000)		No
Seo et al. (2008)	(3)	Fe	⑧[d]	No	$\varepsilon_{tz} = 0.13$ hr u_*[e] in Equation 11	Boxall and Guymer (2003)		Salt concentration (conductivity) measured at 6 locations in 11 sections for five flow configurations in a meandering laboratory channel
			⑥		D_L= 5.93 hr u_* D_T=0.15 hr u_*	Elder (1959) and Fischer et al. (1979)		
Liang et al. (2010)	(3)	Fd, 2nd	⑥	Yes	D_L= 13 hr u_* D_T=1.2 hr u_*	Allegedly Falconer (1991)[f]		No

Water Resources Research

10.1029/2023WR035053

Table 2
Continued

Reference	Equation	Scheme and order[a]	Diffusivity approach (Table 1)	Model verification against analytical solution	Source of diffusivity values			Independent validation by
					Values	Literature data[b]	Calibrated values	Comparison with independent measurements
Park et al. (2016)	(3)	Fe	⑥	No	D_L= 5.93 hr u_* D_T=0.15 hr u_*	Elder (1959) and Fischer et al. (1979)		No
Park and Song (2018)	(3)	Fe	⑥	No	D_L= 5.93 hr u_* D_T=0.6 hr u_*	Elder (1959) and Fischer et al. (1979)		No
Fang et al. (2022)	LHS: (3) RHS: (5)	Fv, 2nd	② ⑥	Yes	$D_L = D_T = 13hu_*$ $D_L = 13hu_*$ $D_T = 1.2hu_*$	Allegedly Falconer (1991)[f]		No
e. Diffusivity coefficients derived from experimental or field concentration measurements								
Ye and McCorquodale (1997)	(3)	Fv, 2nd	③[c]	No	$\sigma_c = 0.15$	As initial guess: Rodi (1984)	Best-fit (trial and error) against meandering laboratory channel data (Chang, 1971)	No
Piasecki and Katopodes (1999)	(3)	Fe, 4th	⑤	No	D_L= 55 m^2/s D_T = 0.75 m^2/s		Best-fit (nonlinear optimization using adjoint sensitivity method) against Potomac River data (Hinz et al., 1989)	No
Duan (2004)	LHS: (3) RHS: (5)	Fe, 2nd	③[c]	No	$\sigma_c = 0.02$		Best-fit (trial and error) against meandering laboratory channel data from Chang (1971)	No
Lee and Seo (2007)	(3)	Fe	⑤	Yes	Lab. Meander D_L = 0.01 m^2/s D_T = 0.001 m^2/s	As initial guess: $D_x = 5.93\ hu_*$ D_y = 0.15–0.6 hu_* from Elder (1959) and Fischer et al. (1979)	Best-fit (trial and error) based on the meandering laboratory open-channel by Baek et al. (2006)	No
					Han river (Korea) D_L=30 m^2/s D_T=0.1 m^2/s		Best-fit (trial and error) based on Han River data (Oct. 2000)	No

Water Resources Research

10.1029/2023WR035053

Table 2
Continued

Reference	Equation	Scheme and order[a]	Diffusivity approach (Table 1)	Model verification against analytical solution	Source of diffusivity values: Values	Source of diffusivity values: Literature data[b]	Source of diffusivity values: Calibrated values	Independent validation by: Comparison with independent measurements
Lee and Seo (2010)	(3)	Fe	⑤	Yes	D_L=30 m^2/s D_T=0.1 m^2/s		Best-fit (trial and error) based on Han River data (Oct. 2000)	No
Hu et al. (2017)	(6)	Fv	③[c]	No	$\sigma_c = 0.125$		Best-fit (trial and error) based on bend-flume laboratory experiments from Chang (1971)	No
Morales-Hernandez et al. (2019)	(3)	Fv, 1st and 2nd	⑥	Yes	$D_L = 5.93\ hu_*$ $D_T = 0.03\ hu_*$		Best fit (systematic sweep) based on laboratory open-channel side cavity data	No
			②		$D_L = 2\ hu_{*L}$[g] $D_T = 2\ hu_{*T}$[g]			
Park et al. (2020)	(3)		⑧[d]	No	$\varepsilon_{tz}(z) = \kappa \frac{z}{h}\left(1 - \frac{z}{h}\right) hu_*$[h] in Equation 11			Salt concentration measured for 12 flow conditions in a laboratory meandering open-channel by Seo and Park (2009)
			⑥		$D_L = [5.11–7.90]\ hu_*$ $D_T = [1.01–2.83]\ hu_*$		Open-channel meandering channel data measured by Seo and Park (2009)	

[a]Numerical scheme (when indicated) with Fd, finite differences; Fe, finite elements; Fv, finite volumes; first, second, third, and fourth indicate the scheme order in space and/or time. [b]Measured data from uniform flow experiments first collected by authors such as Elder (1959), Fischer (1973), Fischer et al. (1979) and recently summarized by Gualtieri and Mucherino (2007), Huai et al. (2018), and Fagour et al. (2022). [c]The turbulent viscosity ν_t was computed with a depth-averaged k-ε model by Ye and McCorquodale (1997); with $\nu_t = \kappa\ h\ u_*/6$ by Duan (2004), κ being the von Karman constant; with an Elder model and a Smagorinsky model by Hu et al. (2017); and presumably with a Smagorinsky model by Wan et al. (2020), as reported by Shen et al. (2016) and by Wang et al. (2018). [d]Seo et al. (2008) and Park et al. (2020) computed the diffusivity tensor as described in Equation 11 using a turbulent diffusivity coefficient ε_{tz} as detailed in the present table. [e]Note that the value $0.13hu_*$ proposed by Boxall and Guymer (2003) is a "transverse mixing coefficient" not a vertical turbulent diffusivity coefficient. [f]This is the citation used by Fang et al. (2022) and Liang et al. (2010) to support their choice of the values of diffusivity coefficients, but we could not find these values in the cited reference (Falconer, 1991). [g]The diffusion tensor involves a single coefficient, but it considers a directional friction model. [h]Notation z represents the elevation above the bed and κ is the von Karman constant.

for Falconer (1986) or Seo et al. (2008), among many others, or (b) calibrate the diffusivity coefficients based on available laboratory data (Morales-Hernandez et al., 2019; Park et al., 2020). For approach ⑦, the diffusivity coefficient values, including the off-diagonal terms, are "arbitrarily selected" by Lee and Kim (2012). For approach ⑧, the method initially proposed by Fischer (1978), was used by Park et al. (2020) and Seo et al. (2008) to evaluate the coefficients of the diffusivity tensor based on a known distribution of horizontal flow velocity over the flow layer, obtained either from measurements or from computational modeling. The formulation involves a depth-integration of the vertical profile of velocity components:

$$D_x = \frac{1}{h}\int_0^h \left\{ \left[\overline{u}(x,y,z) - U(x,y)\right] \int_0^z \left[\frac{1}{\varepsilon_{tz}(x,y,\zeta)} \int_0^\zeta \left[\overline{u}(x,y,\xi) - U(x,y)\right] d\xi \right] d\zeta \right\} dz \tag{11a}$$

$$D_y = \frac{1}{h}\int_0^h \left\{ \left[\overline{v}(x,y,z) - V(x,y)\right] \int_0^z \left[\frac{1}{\varepsilon_{tz}(x,y,\zeta)} \int_0^\zeta \left[\overline{v}(x,y,\xi) - V(x,y)\right] d\xi \right] d\zeta \right\} dz \tag{11b}$$

$$D_{xy} = \frac{1}{h}\int_0^h \left\{ \left[\overline{u}(x,y,z) - U(x,y)\right] \int_0^z \left[\frac{1}{\varepsilon_{tz}(x,y,\zeta)} \int_0^\zeta \left[\overline{v}(x,y,\xi) - V(x,y)\right] d\xi \right] d\zeta \right\} dz \tag{11c}$$

$$D_{yx} = \frac{1}{h}\int_0^h \left\{ \left[\overline{v}(x,y,z) - V(x,y)\right] \int_0^z \left[\frac{1}{\varepsilon_{tz}(x,y,\zeta)} \int_0^\zeta \left[\overline{u}(x,y,\xi) - U(x,y)\right] d\xi \right] d\zeta \right\} dz \tag{11d}$$

where ε_{tz} is the local vertical turbulent diffusivity coefficient, z is the elevation above the bed, h is the flow depth and $\overline{u} - U$ and $\overline{v} - V$ the deviations of local horizontal velocity components compared to the corresponding depth-averaged values. It is interesting to notice the appearance of cross-dispersion terms brought by the depth averaging, even in cases with a local diffusivity tensor ε_t strictly diagonal. Indeed, following the works of Taylor (1954) in pipe flows and of Elder (1959) in 1D open-channels, Fischer et al. (1979) showed that the second-order z-derivative of the local concentration is proportional to the gradients of the depth-average concentration along x and y axes (see their Equation 4.1.10), leading to Equation 11. Several strategies have been used for evaluating the vertical distribution of the two velocity components necessary for the evaluation of Equation 11. A first one consists in using existing field or laboratory measurements of 3D flow velocity, as performed by Park et al. (2020) and Seo et al. (2008). In another strategy, the velocity field can be derived by combining a computed 2D depth-averaged velocity field (as predicted by the shallow-water equations) with empirical or analytical formulas to describe the vertical distribution of the horizontal velocity components. For a flow in a bend channel, Park et al. (2020) used a logarithmic profile for the streamwise velocity component and tested several ad hoc equations for describing the vertical distribution of the transverse velocity component. The authors selected the formula proposed by Odgaard (1986). In a third strategy, not identified in the present review, the velocity field may be computed by a 3D computational model. Park et al. (2020) indicate that using approach ⑧ with Equation 11 to estimate the local diffusion tensor can be successfully applied even when the tracer cloud passes through a locally three-dimensional mixing region, and hence, overcomes the intrinsic restriction of the 2D approach. As such, Equation 11 in approach ⑧ has the potential to overcome limitations of the other approaches listed in Table 1, at the expense of retrieving sufficient information on the vertical profile of the horizontal velocity components. Such measurement is challenging, especially for a field application, but thanks to fast advances in field monitoring technology in recent decades, vertical profile of the horizontal velocity components can now be efficiently acquired using ADCP (e.g., Jung et al., 2019; Shin et al., 2020). Nevertheless, Equation 11 considers only the dispersion induced by the non-uniform distribution over the depth of flow velocity and scalar concentration (term T3 in Equation 1). Considering only this term to estimate the whole diffusivity tensor assumes that turbulent diffusion and mixing due to irregularities and complex roughness of the bed are negligible. For meandering open channels, Lee and Kim (2012) and Park et al. (2020) justify this assumption by the large curvature of the flow and thus the strong secondary currents. According to Fischer et al. (1979), this explains why the longitudinal

dispersion coefficient derived theoretically by Elder (1959) is very low compared to mixing coefficients reported by river studies. Very few quantitative validations of this so-called "velocity-based" method (by comparing the resulting dispersion coefficients with the diffusivity—or mixing-coefficients obtained by scalar release, often labeled "concentration" or "routing" method) could be found in the literature. Moreover, the results of these comparisons are highly disparate. Jung et al. (2019) indicate that neglecting the turbulent diffusion (term T2 in Equation 1) underestimates by only 30% the transverse mixing coefficient in the downstream branch of their open-channel confluence. Oppositely Shin et al. (2020) report transverse and longitudinal dispersion coefficients (with Equation 11) more than four times lower than the, respectively, transverse and longitudinal diffusivity coefficients obtained by a concentration method. More work seems to be required before concluding regarding the applicability of this velocity-based method.

4. Discussion

4.1. Selection and Justification of Diffusivity Coefficients

Table 1 indicates that several approaches can be adopted to evaluate the diffusivity tensor, based on one, two, three, or four coefficients. These coefficients can be of different natures: either dimensional diffusivity value(s), or nondimensional coefficient(s) describing the ratio of diffusivity to hu_* (Elder approach), or a turbulent Schmidt number. Although, Table 2 reveals that some studies simply neglected the diffusivity tensor (two out of 28 reviewed articles in section a of Table 2) or did not report the values of diffusivity considered for the application of their models (five out of 28 reviewed articles in section b). Six other articles report the values used for the diffusivity coefficients, but they do not provide any supporting information for justifying the selected values (section c). Conversely, two methods for justifying the diffusivity coefficient values have been embraced by, respectively, seven (section d) and eight (section e) of the articles reviewed here.

As detailed in section d of Table 2, the first method consists in using coefficients taken from published data sets, such as provided by Elder (1959), Fischer (1973), or Fischer et al. (1979), among other more recent works as that from Seo et al. (2016). Such data are readily available from recent review articles such as Kashefipour and Falconer (2002), Gualtieri and Mucherino (2007), Y. Wang and Huai (2016), Huai et al. (2018), or Fagour et al. (2022). An advantage of this method is that the coefficient values benefit from a long history of measurements (since Elder, 1959) and it is thus possible to select the configuration that suits best the flow characteristics of a particular study (width-to-depth ratio, bed roughness, sinuosity …). The method is simple to implement as it does not demand additional experimental work to calibrate the coefficients, either for laboratory channel or river applications.

In the second method (section e in Table 2), the diffusivity coefficients or Schmidt numbers are calibrated so that computed concentration outcomes match measured data. Most studies used trial and error to conduct the calibration, with only two exceptions. Piasecki and Katopodes (1999) use a nonlinear optimization algorithm-based adjoint sensitivity method, while Morales-Hernandez et al. (2019) systematically scan a range of plausible values. The observations used for this calibration are taken from scalar mixing experiments performed either in laboratory setups by Chang (1971), Baek et al. (2006), Seo and Park (2009) or Morales-Hernandez et al. (2019), or in field conditions by Hinz et al. (1989) or Lee and Seo (2007).

Besides, Park et al. (2020) and Seo et al. (2008) adopt an analytical method (Equation 11) to compute the diffusivity tensor (using the Von Karman constant, the water depth, and the friction velocity) which either does not require any empirical coefficient (Park et al., 2020) or requires an empirical coefficient to estimate the vertical turbulent diffusivity coefficient (Seo et al., 2008). Still, the applicability of this method remains an open question.

Note finally, that, added to the computed diffusion-dispersion term, a numerical diffusion inherent to any numerical model acts in all calculations presented here. For the most precise numerical schemes (of higher order, see Table 2), this numerical diffusion is reduced and the contribution of the diffusion-dispersion term dominates. Oppositely, for the lowest order schemes (typically of order 1) both the diffusion-dispersion term and numerical diffusion affect the concentration results.

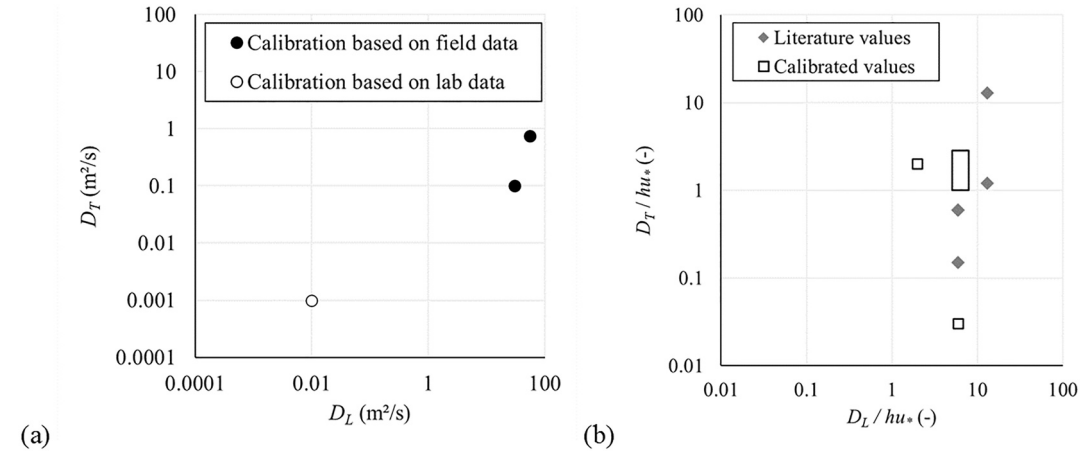

Figure 1. Values of the diffusivity coefficients either retrieved from the literature data or calibrated. (a) Dimensional diffusivity coefficients; (b) nondimensional coefficients describing the ratio of diffusivity to hu_* (Elder approach).

4.2. Values of the Diffusivity Coefficients

Values of diffusivity coefficients obtained by calibration against measured concentrations (section e in Table 2) are summarized in Figure 1, as well as in Table 3 together with calibrated values of the Schmidt number. Overall, the calibrated values differ considerably from one study to the other.

Duan (2004), Hu et al. (2017), Ye and McCorquodale (1997) identify values of the Schmidt number using the same laboratory data set, namely scalar mixing measurements in a meandering channel performed by Chang (1971). Nonetheless, the calibrated values of σ_c vary significantly: $\sigma_c = 0.15$, 0.02, and 0.125 are found by Duan (2004), Hu et al. (2017), and Ye and McCorquodale (1997), respectively. The lower Schmidt number value selected by Duan (2004) is attributed to the use of a simpler turbulence model (Elder formula) compared to the depth-averaged k-ε model used by Ye and McCorquodale (1997). It is acknowledged that the Schmidt number needs to be recalibrated because its value depends on the accuracy of the flow model and associated turbulence closure. In contrast, Hu et al. (2017) do not refer to the previous studies and they do not discuss possible explanations for a mismatch between calibrated values of the Schmidt number.

Lee and Seo (2007, 2010) and Piasecki and Katopodes (1999) calibrate dimensional diffusivity coefficients using field data (Table 3 and Figure 1a). The calibrated values fall in ranges consistent with other studies such as $D_L \sim$ (5–1,000) m²/s as reported by Kashefipour and Falconer (2002) and Y. Wang and Huai (2016) for the longitudinal diffusivity coefficient and $D_T \sim$ (0.01–1) m²/s as reported by Huai et al. (2018) for the transverse coefficient.

Values of nondimensional coefficients describing the ratio of diffusivity to hu_* (Elder approach) are calibrated based on laboratory data by Morales-Hernandez et al. (2019) and Park et al. (2020). The values obtained for the longitudinal coefficient D_L/hu_* (Table 3 and Figure 1b) fall in a range consistent with previous literature data, that is, typically $D_L/hu_* \sim$ (5–15) (Elder, 1959; Fischer, 1973). For the transverse coefficient, D_T/hu_*, calibrated values in the range (1.01–2.83) are found by Seo and Park (2009) and reused by Park et al. (2020), which appears gener-

Table 3
Values of the Diffusivity Coefficients and Schmidt Number Extracted From the Literature Data or Calibrated Based on Measured Scalar Concentrations

		Dimensional diffusivity coefficients (m²/s)		Nondimensional coefficients (–)		Schmidt number (–)
		D_L	D_T	D_L/hu_*	D_T/hu_*	σ_c
From literature (section d in Table 2)				5.93	0.15, 0.6	
				13	1.2, 13	
Calibrated (section e in Table 2)	Laboratory data	10^{-2}	10^{-3}	5.93, [5.11–7.90]	0.03, [1.01–2.83]	0.02, 0.125, 0.15
	Field data	30	0.1			
		55	0.75			

ally consistent with values previously reported in literature such as $D_T/hu_* \sim (0.5–2)$ in bend channels according to Fischer (1973). In contrast, the value of $D_T/hu_* = 0.03$ calibrated by Morales-Hernandez et al. (2019) appears way smaller than previously reported values, even in straight channels (e.g., $D_T/hu_* \sim [0.1–0.25]$ according to Huai et al., 2018). Based on a velocity field measured in a shallow meandering experimental channel, Lee and Seo (2013) used Equation 11 to estimate local diffusivity values $D_L/hu_* = (0.6–9.42)$ and $D_T/hu_* = (0.1–3.5)$.

4.3. Validation of Diffusivity Coefficient Values

Table 2 reveals that, irrespective of the method used for estimating the coefficients in the diffusivity tensor very few authors validate their selection of diffusivity coefficients based on independent measurements. The validation attempts in Table 2 appear for diffusivity coefficients taken from the literature or analytical data, but no author validates the coefficients after calibration on another set of measured data.

Lin and Falconer (1997) compare the predicted and measured sediment flux in an estuary in the UK. Wan et al. (2020) compare their calculations with four total dissolved gas saturation data measured in a Chinese river. Falconer (1986) validates his calculations based on 24 measured nitrogen concentrations in an inland basin in the UK. However, in these three studies, the appraisal of model performance in the validation phase remains qualitative.

Park et al. (2020) and Seo et al. (2008) compare predicted and measured salt concentrations along the centerline of a double meander laboratory channel with smooth rectangular cross-section (still both experimental set-ups being different from each other). Seo et al. (2008) conclude that adopting approach ⑧ together with Equation 11 produces more accurate results than computations based on approach ⑥ with diffusivity coefficients taken from the literature (Table 1), especially for reproducing scalar mixing in the transverse direction. According to Park et al. (2020), although substantial discrepancies between computed and observed concentrations are found in the upstream bend (because the vertical mixing of the tracer cloud is not complete at the scalar released point), the errors in the computed peak concentration and arrival time decrease after the first bend when approach ⑧ is used with Equation 11, because Equation 11 enables accounting for the spanwise variations of shear dispersion.

5. Conclusion

Computing the transport of a passive tracer within shallow open-channel flows is of major importance for evaluating the risk of pollution in natural and anthropic water systems and for guiding protection strategies. Moreover, it enables simulating the transport of gazes or other chemicals naturally present in the water. In this article, we highlight the broad diversity of mathematical formulations and diffusivity tensor parametrizations used so far for a depth-averaged Eulerian modeling of scalar transport and mixing in shallow flows. To the best of the author's knowledge, similar reviews exist for 3D models (Gualtieri et al., 2017) but not for depth-averaged 2D models.

Among the 28 reviewed studies, seven different formulations of the 2D advection-diffusion equation could be identified, as well as eight distinct approaches for estimating the corresponding diffusivity tensor. In 20 out of the 28 reviewed studies, the 2D advection-diffusion equation is formulated consistently with the depth-integration of the 3D advection-diffusion equation. Surprisingly, some authors use model formulations that appear not to result from a proper depth-integration, and as such these models seem not to be valid in the presence of substantial variations in flow depth across the considered domain.

Quantifying the diffusivity tensor is particularly challenging as it lumps multiple processes which influence scalar dispersion, that is, molecular diffusion, turbulent diffusion as well as dispersion induced by complex velocity and concentration profiles over the flow layer, including the effects of secondary currents. Depending on the studies, the number of coefficients to be identified for evaluating the diffusivity tensor varies between one and four, depending on whether the tensor is assumed isotropic or not. These coefficients are of three types: either dimensional diffusivity values, nondimensional coefficients in an Elder-type formulation, or as a Schmidt number. Besides, our findings shown in Table 1 suggest that some tensor formulations have remained unexplored, such as a nonisotropic extension of approach ③ (Duan, 2004; Hu et al., 2017; Ye & McCorquodale, 1997), in which distinct values of the Schmidt number would be assigned to the streamwise and crosswise directions, leading to a new formulation analogous to approaches ⑤ or ⑥ but involving Schmidt numbers.

The reviewed studies provide contrasting levels of detail regarding the choice and justification of the diffusivity coefficient values. Seven studies either neglect or do not report the considered diffusivity values, and six others use arbitrarily selected values. In seven other studies, the diffusivity values are taken from the literature of scalar dispersion in open channels and rivers, that is, mostly from Elder (1959), Fischer (1973), or Fischer et al. (1979). Only eight studies use laboratory or field measurements for calibrating the diffusivity coefficients, and two of them adopted an analytical approach (Equation 11) to derive the diffusivity coefficients from observed or assumed flow velocity profiles over the flow depth. Among them, solely Park et al. (2020) conducted independent validation of the model outcome after the calibration phase.

An alternative way to compute a scalar dispersion in a 2D shallow flow is to apply a Lagrangian approach (e.g., Palman et al., 2021; Park & Seo, 2018), which is out of the scope of the present review. In this case, diffusion and dispersion effects are accounted for through a random component, which may be considered either as isotropic (Sämann et al., 2019) or nonisotropic (Jiang et al., 2021).

To further advance our modeling capacity of scalar transport and dispersion in shallow environmental flow, it is of utmost importance that future research systematically provides a transparent reporting and justification of the considered values of the components of the diffusivity tensor. Research on the topic would also benefit from the generalization of a two-step procedure, in which the diffusivity tensor is first calibrated, and then evaluated against independent data in a so-called validation phase, as it is standard in other fields of environmental engineering or water resources management such as stream flow modeling. Validation is instrumental to allow assessing the generalization errors and the transferability of diffusivity coefficients identified in a particular flow setting. However, mainstreaming such an evaluation of model performance is critically dependent on the availability of high-quality and extensively documented observation data sets.

Data Availability Statement

No data were produced for this review article and all data used for the single figure were taken directly from the cited articles.

Acknowledgments
The authors wish to thank the reviewers and associate editor for their contributions during the review process, which permitted to improve the quality of the manuscript.

References

Addison-Atkinson, W., Chen, A. S., Memon, F. A., & Chang, T. J. (2022). Modelling urban sewer flooding and quantitative microbial risk assessment: A critical review. *Journal of Flood Risk Management*, *15*(4), e12844. https://doi.org/10.1111/jfr3.12844

Alavian, V. (1986). Dispersion tensor in rotating flows. *Journal of Hydraulic Engineering*, *112*(8), 771–777. https://doi.org/10.1061/(asce)0733-9429(1986)112:8(771)

Baek, K. O., & Seo, I. W. (2010). Routing procedures for observed dispersion coefficients in two-dimensional river mixing. *Advances in Water Resources*, *33*(12), 1551–1559. https://doi.org/10.1016/j.advwatres.2010.09.005

Baek, K. O., Seo, I. W., & Jeong, S. J. (2006). Evaluation of dispersion coefficient in meandering channels from transient tracer tests. *Journal of Hydraulic Engineering*, *132*(10), 1021e1032.

Behzadi, F., Shamsaei, B., & Newman, J. C., III. (2018). Solution of fully-coupled shallow water equations and contaminant transport using a primitive-variable Riemann method. *Environmental Fluid Mechanics*, *18*(2), 515–535. https://doi.org/10.1007/s10652-017-9571-7

Boxall, J. B., & Guymer, I. (2003). Analysis and prediction of transverse mixing coefficients in natural channels. *Journal of Hydraulic Engineering*, *129*(2), 129–139. https://doi.org/10.1061/(asce)0733-9429(2003)129:2(129)

British Transport Docks Board. (1980). Humber estuary sediment flux, part I: field measurements. Rep. No. 283, Middlesex, England (p. 91).

Chang, Y. C. (1971). Lateral mixing in meandering channels. (PhD thesis). University of Iowa.

Cheng, R. T., Casulli, V., & Milford, S. N. (1984). Eulerian-Lagrangian solution of the convection-dispersion equation in natural coordinates. *Water Resources Research*, *20*(7), 944–952. https://doi.org/10.1029/wr020i007p00944

De Barros, F. P. J., Mills, W. B., & Cotta, R. M. (2006). Integral transform solution of a two-dimensional model for contaminant dispersion in rivers and channels with spatially variable coefficients. *Environmental Modelling & Software*, *21*(5), 699–709. ISSN 1364-8152. https://doi.org/10.1016/j.envsoft.2005.02.002

Duan, J. G. (2004). Simulation of flow and mass dispersion in meandering channels. *Journal of Hydraulic Engineering*, *130*(10), 964–976. https://doi.org/10.1061/(asce)0733-9429(2004)130:10(964)

Elder, J. (1959). The dispersion of marked fluid in turbulent shear flow. *Journal of Fluid Mechanics*, *5*(4), 544–560. https://doi.org/10.1017/s0022112059000374

Fagour, C., Gond, L., Le Coz, J., Riviere, N., Gostiaux, L., Mignot, E., & Kateb, L. (2022). Transverse mixing coefficients in non-uniform flows: Laboratory experiments. In *Proceedings of the 39th IAHR World Congress, 19–24 June 2022*.

Falconer, R. A. (1986). A two-dimensional mathematical model study of the nitrate levels in an inland natural basin. *International Conference on Water Quality Modelling in the Inland Natural Environment* (pp. 325–344).

Falconer, R. A. (1991). Review of modelling flow and pollutant transport processes in hydraulic basins. *Water Pollution: Modelling, Measuring and Prediction*, 3–23. https://doi.org/10.1007/978-94-011-3694-5_1

Fang, S., Ji, Y., & Zhang, M. (2022). Numerical modeling the flood and pollutant transport processes in residential areas with different land use types. *Advances in Meteorology*, *2022*, 1–16. https://doi.org/10.1155/2022/9320089

Fernández-Pato, J., & García-Navarro, P. (2021). An efficient GPU implementation of a coupled overland-sewer hydraulic model with pollutant transport. *Hydrology*, *8*(4), 146. https://doi.org/10.3390/hydrology8040146
Ferziger, J. H., & PeriC, M. (2002). *Computational methods for fluid dynamics*. Springer Berlin.
Fischer, H. B. (1973). Longitudinal dispersion and turbulent mixing in open-channel flow. *Annual Review of Fluid Mechanics*, *5*(1), 59–78. https://doi.org/10.1146/annurev.fl.05.010173.000423
Fischer, H. B. (1978). On the tensor form of the bulk dispersion coefficient in a bounded skewed shear flow. *Journal of Geophysical Research*, *83*(C5), 2373–2375. https://doi.org/10.1029/jc083ic05p02373
Fischer, H. B., List, E. J., Koh, R. C. Y., Imberger, J., & Brooks, N. H. (1979). *Mixing in inland and coastal waters*. Academic.
Gond, L., Mignot, E., Le Coz, J., & Kateb, L. (2021). Transverse mixing in rivers with longitudinally varied morphology. *Water Resources Research*, *57*(6), e2020WR029478. https://doi.org/10.1029/2020wr029478
Gualtieri, C. (2010). RANS-based simulation of transverse turbulent mixing in a 2D geometry. *Environmental Fluid Mechanics*, *10*(1), 137–156. https://doi.org/10.1007/s10652-009-9119-6
Gualtieri, C., Angeloudis, A., Bombardelli, F., Jha, S., & Stoesser, T. (2017). On the values for the turbulent Schmidt number in environmental flows. *Fluids*, *2*(2), 17. https://doi.org/10.3390/fluids2020017
Gualtieri, C., & Mucherino, C. (2007). 5th International Symposium on Environmental Hydraulics (ISEH 2007), Tempe, USA.
Hinz, S., Katopodes, N. D., Freedman, P., Sullivan, M. P., & Freudberg, S. A. (1989). A FEM model for non-conservative plumes in the Potomac River.' In *Estuarine and coastal modeling* (pp. 233–240). ASCE.
Hu, D., Zhu, Y., Zhong, D., & Qin, H. (2017). Two-dimensional finite-volume Eulerian-Lagrangian method on unstructured grid for solving advective transport of passive scalars in free-surface flows. *Journal of Hydraulic Engineering*, *143*(12), 04017051. https://doi.org/10.1061/(asce)hy.1943-7900.0001371
Huai, W., Shi, H., Yang, Z., & Zeng, Y. (2018). Estimating the transverse mixing coefficient in laboratory flumes and natural rivers. *Water, Air. & Soil Pollution*, *229*(8), 1–17.
Jackson, T. R., Haggerty, R., & Apte, S. V. (2013). A fluid-mechanics based classification scheme for surface transient storage in riverine environments: Quantitatively separating surface from hyporheic transient storage. *Hydrology and Earth System Sciences*, *17*(7), 2747–2779. https://doi.org/10.5194/hess-17-2747-2013
Jiang, J., Liang, Q., Xia, X., & Hou, J. (2021). A coupled hydrodynamic and particle-tracking model for full-process simulation of nonpoint source pollutants. *Environmental Modelling & Software*, *136*, 104951. https://doi.org/10.1016/j.envsoft.2020.104951
Jung, S. H., Seo, I. W., Kim, Y. D., & Park, I. (2019). Feasibility of velocity-based method for transverse mixing coefficients in river mixing analysis. *Journal of Hydraulic Engineering*, *145*(11), 04019040. https://doi.org/10.1061/(asce)hy.1943-7900.0001638
Kashefipour, S. M., & Falconer, R. A. (2002). Longitudinal dispersion coefficients in natural channels. *Water Research*, *36*(6), 1596–1608. https://doi.org/10.1016/s0043-1354(01)00351-7
Lau, Y. L., & Krishnappan, B. G. (1977). Transverse dispersion in rectangular channel. *Journal of the Hydraulics Division*, *103*(HY10), 1173–1189. https://doi.org/10.1061/jyceaj.0004851
Lee, M. E., & Kim, G. (2012). Influence of secondary currents on solute dispersion in curved open channels. *Journal of Applied Mathematics*, *2012*. https://doi.org/10.1155/2012/781695
Lee, M. E., & Seo, I. W. (2007). Analysis of pollutant transport in the Han River with tidal current using a 2D finite element model. *Journal of Hydro-Environment Research*, *1*(1), 30–42. https://doi.org/10.1016/j.jher.2007.04.006
Lee, M. E., & Seo, I. W. (2010). 2D finite element pollutant transport model for accidental mass release in rivers. *KSCE Journal of Civil Engineering*, *14*(1), 77–86. https://doi.org/10.1007/s12205-010-0077-9
Lee, M. E., & Seo, I. W. (2013). Spatially variable dispersion coefficients in meandering channels. *Journal of Hydraulic Engineering*, *139*(2), 141–153. https://doi.org/10.1061/(asce)hy.1943-7900.0000669
Li, S., & Duffy, C. J. (2012). Fully-coupled modeling of shallow water flow and pollutant transport on unstructured grids. *Procedia Environmental Sciences*, *13*, 2098–2121. https://doi.org/10.1016/j.proenv.2012.01.200
Liang, D., Wang, X., Falconer, R. A., & Bockelmann-Evans, B. N. (2010). Solving the depth-integrated solute transport equation with a TVD-MacCormack scheme. *Environmental Modelling & Software*, *25*(12), 1619–1629. https://doi.org/10.1016/j.envsoft.2010.06.008
Lin, B., & Falconer, R. A. (1997). Tidal flow and transport modeling using ULTIMATE QUICKEST scheme. *Journal of Hydraulic Engineering*, *123*(4), 303–314. https://doi.org/10.1061/(asce)0733-9429(1997)123:4(303)
Mark, O., Jørgensen, C., Hammond, M., Khan, D., Tjener, R., Erichsen, A., & Helwigh, B. (2018). *A new methodology for modelling of health risk from urban flooding exemplified by cholera—Case Dhaka, Bangladesh* (pp. 28–42). Blackwell Publishing Inc.
Morales-Hernandez, M., Murillo, J., & Garcia-Navarro, P. (2019). Diffusion-dispersion numerical discretization for solute transport in 2D transient shallow flows. *Environmental Fluid Mechanics*, *19*(5), 1217–1234. https://doi.org/10.1007/s10652-018-9644-2
Murillo, J., Garcia-Navarro, P., Burguete, J., & Brufau, P. (2006). A conservative 2D model of inundation flow with solute transport over dry bed. *International Journal for Numerical Methods in Fluids*, *52*(10), 1059–1092. https://doi.org/10.1002/fld.1216
Odgaard, A. J. (1986). Meander flow model. I: Development. *Journal of Hydraulic Engineering*, *112*(12), 1117–1136. https://doi.org/10.1061/(asce)0733-9429(1986)112:12(1117)
Palman, L. E., Trento, A. E., & Alvarez, A. M. (2021). Scalar dispersion in the Salado River through tracers test and two-dimensional model. *Water, Air, & Soil Pollution*, *232*(12), 1–16. https://doi.org/10.1007/s11270-021-05436-1
Park, I., & Seo, I. W. (2018). Modeling non-Fickian pollutant mixing in open channel flows using two-dimensional particle dispersion model. *Advances in Water Resources*, *111*, 105–120. https://doi.org/10.1016/j.advwatres.2017.10.035
Park, I., Seo, I. W., Do Kim, Y., & Song, C. G. (2016). Flow and dispersion analysis of shallow water problems with Froude number variation. *Environmental Earth Sciences*, *75*(2), 1–12. https://doi.org/10.1007/s12665-015-4928-z
Park, I., Seo, I. W., Shin, J., & Song, C. G. (2020). Experimental and numerical investigations of spatially-varying dispersion tensors based on vertical velocity profile and depth-averaged flow field. *Advances in Water Resources*, *142*, 103606. https://doi.org/10.1016/j.advwatres.2020.103606
Park, I., & Song, C. G. (2018). Analysis of two-dimensional flow and pollutant transport induced by tidal currents in the Han River. *Journal of Hydroinformatics*, *20*(3), 551–563. https://doi.org/10.2166/hydro.2017.118
Pathirana, A., Maheng Dikman, M., & Brdjanovic, D. (2011). A two dimensional pollutant transport model for sewer overflow impact simulation. In *Proceedings: 12th International Conference on Urban Drainage, Porto Alegre/Brazil* (pp. 10–15).
Piasecki, M., & Katopodes, N. D. (1999). Identification of stream dispersion coefficients by adjoint sensitivity method. *Journal of Hydraulic Engineering*, *125*(7), 714–724. https://doi.org/10.1061/(asce)0733-9429(1999)125:7(714)
Sämann, R., Graf, T., & Neuweiler, I. (2019). Modeling of contaminant transport during an urban pluvial flood event—The importance of surface flow. *Journal of Hydrology*, *568*, 301–310. https://doi.org/10.1016/j.jhydrol.2018.10.002

Seo, I. W., Choi, H. J., Kim, Y. D., & Han, E. J. (2016). Analysis of two-dimensional mixing in natural streams based on transient tracer tests. *Journal of Hydraulic Engineering*, *142*(8), 04016020. https://doi.org/10.1061/(asce)hy.1943-7900.0001118

Seo, I. W., Lee, M. E., & Baek, K. O. (2008). 2D modeling of heterogeneous dispersion in meandering channels. *Journal of Hydraulic Engineering*, *134*(2), 196–204. https://doi.org/10.1061/(asce)0733-9429(2008)134:2(196)

Seo, I. W., & Park, S. W. (2009). Effects of velocity structures on tracer mixing in a meandering channel. *Journal of the Korean Society of Civil Engineering*, *29*(1B), 35–45. (In Korean).

Shen, X., Li, R., Huang, J., Feng, J., Hodges, B. R., Li, K., & Xu, W. (2016). Shelter construction for fish at the confluence of a river to avoid the effects of total dissolved gas supersaturation. *Ecological Engineering*, *97*, 642–648. https://doi.org/10.1016/j.ecoleng.2016.10.055

Shin, J., Seo, I. W., & Baek, D. (2020). Longitudinal and transverse dispersion coefficients of 2D contaminant transport model for mixing analysis in open channels. *Journal of Hydrology*, *583*, 124302. https://doi.org/10.1016/j.jhydrol.2019.124302

Taylor, G. I. (1954). The dispersion of matter in turbulent flow through a pipe. In *Proceedings of the Royal Society of London. Series A. Mathematical and Physical Sciences* (Vol. 223(1155), pp. 446–468).

Wan, H., Li, J., Li, R., Feng, J., & Sun, Z. (2020). The optimal power generation operation of a hydropower station for improving fish shelter area of low TDG level. *Ecological Engineering*, *147*, 105749. https://doi.org/10.1016/j.ecoleng.2020.105749

Wang, H., Li, Y., Li, J., An, R., Zhang, L., & Chen, M. (2018). Influences of hydrodynamic conditions on the biomass of benthic diatoms in a natural stream. *Ecological Indicators*, *92*, 51–60. https://doi.org/10.1016/j.ecolind.2017.05.061

Wang, Y., & Huai, W. (2016). Estimating the longitudinal dispersion coefficient in straight natural rivers. *Journal of Hydraulic Engineering*, *142*(11), 04016048. https://doi.org/10.1061/(asce)hy.1943-7900.0001196

Ye, J., & McCorquodale, J. A. (1997). Depth-averaged hydrodynamic model in curvilinear collocated grid. *Journal of Hydraulic Engineering*, *123*(5), 380–388. https://doi.org/10.1061/(asce)0733-9429(1997)123:5(380)

Zhang, L., Liang, Q., Wang, Y., & Yin, J. (2015). A robust coupled model for solute transport driven by severe flow conditions. *Journal of Hydro-Environment Research*, *9*(1), 49–60. https://doi.org/10.1016/j.jher.2014.04.005

References From the Supporting Information

Ouro, P., Fraga, B., Viti, N., Angeloudis, A., Stoesser, T., & Gualtieri, C. (2018). Instantaneous transport of a passive scalar in a turbulent separated flow. *Environmental Fluid Mechanics*, *18*(2), 487–513. https://doi.org/10.1007/s10652-017-9567-3

Pope, S. B. (2000). *Turbulent flows*. Cambridge University Press.

Rossi, R., & Iaccarino, G. (2009). Numerical simulation of scalar dispersion downstream of a square obstacle using gradient-transport type models. *Atmospheric Environment*, *43*(16), 2518–2531. https://doi.org/10.1016/j.atmosenv.2009.02.044

Shen, X., Li, R., Hodges, B. R., Feng, J., Cai, H., & Ma, X. (2019). Experiment and simulation of supersaturated total dissolved gas dissipation: Focus on the effect of confluence types. *Water Research*, *155*, 320–332. https://doi.org/10.1016/j.watres.2019.02.056

Tavoularis, S., & Corrsin, S. (1985). Effects of shear on the turbulent diffusivity tensor. *International Journal of Heat and Mass Transfer*, *28*(1), 265–276. https://doi.org/10.1016/0017-9310(85)90028-6

Wu, W. (2007). *Computational river dynamics*. CRC Press.